IJST, Transactions of Civil Engineering, Vol. 38, No. C2, pp 359-376
Printed in The Islamic Republic of Iran, 2014

SEISMIC BEHAVIOR OF INTERNAL REINFORCED CONCRETE BEAM-COLUMN JOINTS: A DETAILED MODELING AND SIMULATION INVESTIGATION*

M. LALEHPARVAR[1] AND MO. R. BANAN[2**]

[1,2]Dept. of Civil and Environmental Eng., School of Eng., Shiraz University, Shiraz, 7134851156, I. R. of Iran
Email: banan@shirazu.ac.ir

Abstract– In a Seismic Force Resisting System (SFRS), beam-column joints are crucial structural elements. Failure of these elements may lead to total collapse of a structure. Recent earthquakes have demonstrated that structural systems designed based on current codes of practice are vulnerable to sever damages, mostly due to undesirable performance of joints. In general, design codes do not consider the effects of joint characteristics on the behavior of the structure and treat joints as members which remain elastic during an earthquake. To thoroughly understand the effects of different design parameters on the behavior of beam-column connections in RC structures and consequently on the overall performance of SFRS, a wide range of experiments must be carried out. But prior to a successful setup and conducting any experiments, a theoretical study and numerical simulation is essential. Therefore, having some reliable F.E. models at our disposal plays a significant role in the field of experimental and theoretical research.

This paper first explains, in detail, the process for developing a F.E. model for RC beam-column connections in the simulation environment provided by ANSYS. Next an attempt is made to study the behavior of RC beam-column joints subjected to seismic forces using the developed model. Finally, the effects of main joint characteristics including ductility, moment capacity ratio, type of loading, ultimate loads, over-strength factors and joint transverse reinforcement are investigated.

Keywords– RC joint, ductility, over-strength factor, moment capacity, push-over, cyclic load, seismic force

1. INTRODUCTION

To understand the seismic behavior of reinforced concrete beam-column joints (R.C. B-C) extensive researches have been conducted since the early 1960's. Among the pioneers in this field, Hanson and Conner [1, 2] studied the behavior of joints in Portland Cement Association laboratories. In 1976, ACI-ASCE committee 352 published its first provisions on connection design [3]. Since then the subject has enjoyed greater popularity [4-20]. Each year, the amount of research on this subject grows, providing more and more insight on joint behavior.

In the field of RC connections, retrofitting the RC joints by using FRP layers has also attracted a great deal of attention [21, 24]. Besides, some researchers have been focusing on the studying the behavior of precast RC framed systems [25].

On the other hand, any change in a design philosophy will also affect the design process of joints which consequently demands more investigation on the behavior of joints. The current philosophy for designing joints in reinforced concrete structures is on the basis that joints will remain rigid during any loading pattern and provides requirements to fulfill this assumption [4]. Recent earthquakes in urban areas such as

*Received by the editors July 20, 2013; Accepted February 8, 2014.
**Corresponding author

Northridge (1994), Kobe (1995) and Kocaeli Turkey (1999), demonstrated that the current design philosophy may need a revision.

This paper attempts to study the behavior of reinforced concrete beam-column internal joints under seismic forces using finite element models and compares the results with code requirements. The main goal of this investigation is to roughly realize whether or not the design provisions for RC B-C joints are safe or whether these provisions should be revised.

2. CALIBRATION OF A F.E. MODEL FOR R.C. B-C JOINTS

a) Introduction

In general, having access to a well-equipped laboratory to test full scale structures is the best way to investigate the effects of different parameters on the behavior of a structure. If for any reason access to such a laboratory is not feasible, having a reliable finite element model could also be a reasonable tool to study structural behaviors. This paper studies the behavior of R.C. B-C joints under seismic loads by constructing and using robust F.E. models in a simulation environment.

To do so, the first step is to be assured that the outputs of a developed F.E. model are reliable. To achieve such confidence, the software's essential modeling parameters must be calibrated and verified by experimental measurements.

We thoroughly examined many available numerical and experimental results on the behavior of RC B-C connections reported by a few researchers [5-20]. By careful study of all these tests it was finally concluded that the experimental test setup and the results reported by Murty et al [5] on RC B-C joints are a reliable source for calibration process of our numerical model.

Murty et al [5] studied the effect of joint core reinforcement detailing on seismic behavior of T-joints. Figure 1 shows the details of the test set up and specimen reinforcement.

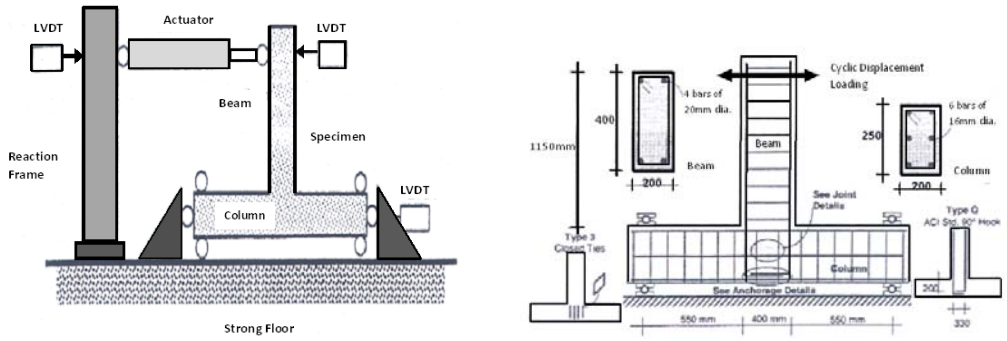

(a) (b)

Fig. 1. (a) Test setup, (b) Layout of the specimen reinforcement [5]

To verify that our F.E. model is appropriately constructed up to our research goal, we adjusted the parameters of the model such that the load-displacement curves developed by the F.E. model properly match with the real curves generated by the experiments.

b) Modeling

To simulate a finite element model with good accuracy there are many parameters to be defined in a software environment, such as geometry, element types, material properties, meshing, loading and analysis type. ANSYS is a user friendly environment which makes this process easy. In the following section some parameters will be defined and adjusted such that the discrepancy between the results from the F.E. model and the real data are minimized.

1. Element type: Choosing a proper element type will lead to a suitable stiffness matrix. By checking the element library of ANSYS, a 3D-8node solid element named "Solid Concrete 65" was chosen.

2. Real constants: In ANSYS reinforcing is characterized by defining some so-called real constants. Figure 2 shows these real constants which are used in our proposed model. Type 1 is used for unreinforced concrete, type 2 for beam longitudinal bars, type 6 for column longitudinal reinforcement and types 3, 4 and 5 for transverse steel. The difference between these types of reinforcement is the orientation and magnitude of the rebars in a concrete element.

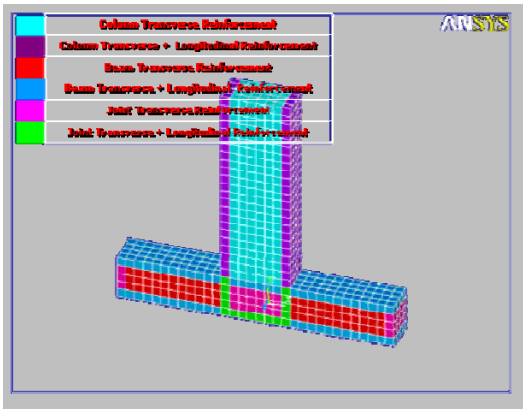

Fig. 2. Real constants defined for a F.E. model developed by ANSYS

3. Materials: To properly simulate concrete behavior, two different material properties: (*i*) nonlinear-inelastic-nonmetal plasticity-concrete and (*ii*) non-linear-inelastic-rate independent- kinematics hardening-Misses plasticity were mixed together. These two material properties are predefined in the program menu. The first parameter models the brittle behavior of concrete with respect to development and propagation of cracks as well as concrete crushing. The second parameter models the concrete post failure behavior. Figure 3 shows the stress-strain curve which is used for concrete in a uni-axial loading situation.

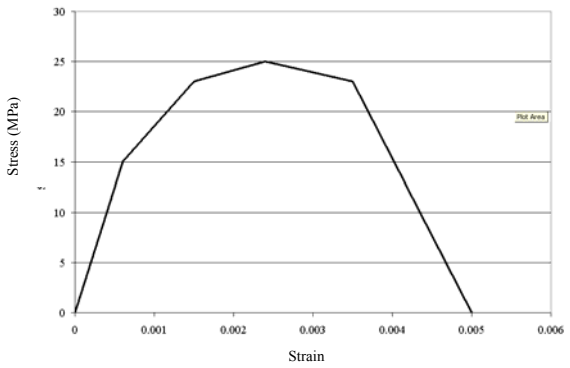

Fig. 3. Stress-Strain curve for concrete

Several parameters must be carefully defined in order to mimic a specific behavior of concrete. Parameters such as the coefficient of shear transform in closed and opened cracks, uni-axial compression stress, uni-axial tension stress, modulus of elasticity and Poisson's ratio. There are well proposed magnitudes for all of these parameters in the literature, except for two shear transformation coefficients. They must be determined by a trial and error procedure. We have broadly investigated the effect of various quantities for these two coefficients and eventually recommend 0.19 and 0.90 for these two coefficients associated with opened and closed crack situations, respectively.

Steel property is defined by: nonlinear-inelastic-rate independent-kinematics hardening-Misses plasticity model which thoroughly simulates the steel behavior. Figure 4 shows the stress-strain curve used for steel rebars for uni-axial loading.

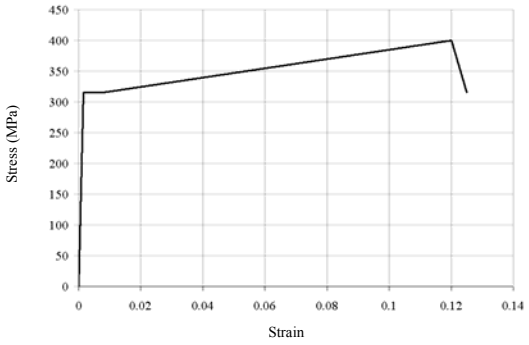

Fig. 4. Stress-Strain curve for steel

To prevent stress concentration and premature failure, an isotropic linear elastic element with high modulus of elasticity (approximately 10 times that of steel modulus) is used near the supports. Figure 5 shows the elements made of this material at supports.

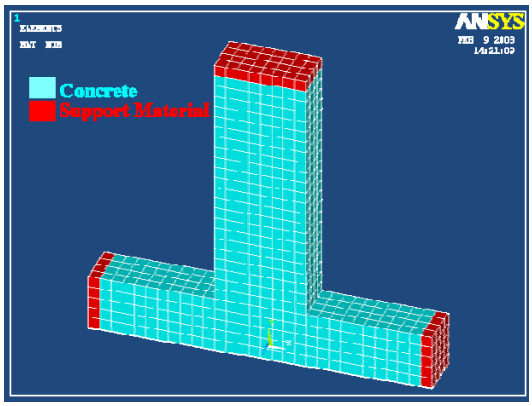

Fig. 5. Elements in the vicinity of supports

4. Loading: Two types of loads are applied to the models: (*i*) pushover loads and (*ii*) cyclic loads. Both loads are displacement-control type with an increasing magnitude. Figure 6 shows cyclic loading pattern used to analyze the models.

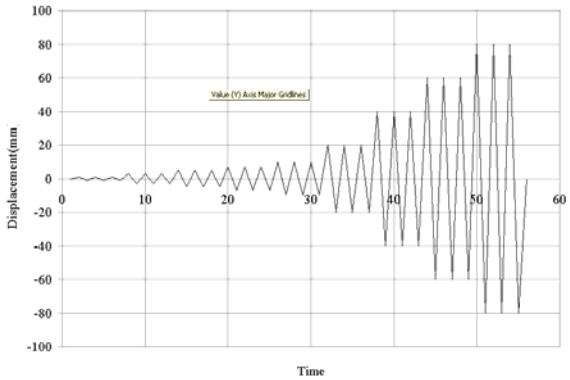

Fig. 6. Pattern of Cyclic loading used in the real test [5]

5. Analysis Type: All the models are analyzed using static pushover analysis and dynamic transient analysis (refers to as cyclic loading). In order to consider the effect of loading rate the analysis is divided into several sub-steps. It is well known that the accuracy of numerical results is sensitive to the number of sub-steps. We have observed that using 20 to 40 sub-steps leads to reasonably good results.

c) Processing the results

After running the program the results can be read in the general post-processor menu. Figures 7 through 11 show the numerical outputs which can be compared with real test results. As shown in Fig. 7, the results of pushover analysis match well with the backbone of the cyclic real test results.

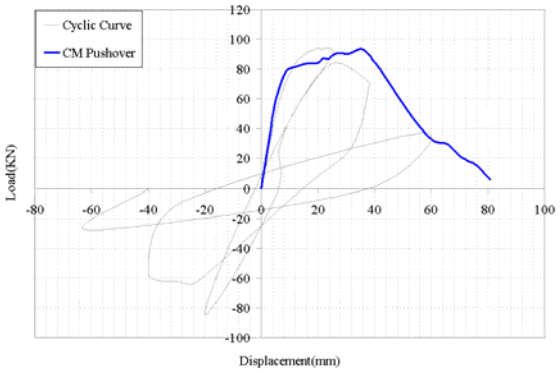

Fig. 7. Pushover result for the simulated model

Figures 8 and 9 show that the results of cyclic analysis match well with both pushover and cyclic real test data.

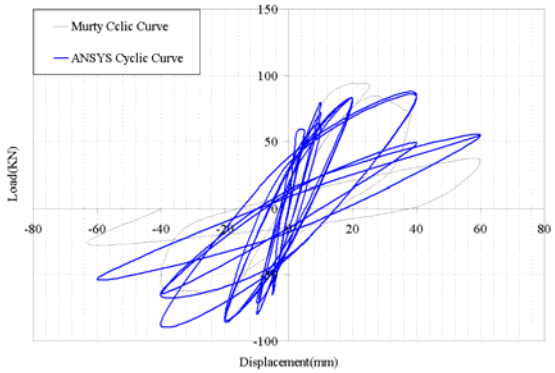

Fig. 8. Cyclic results from the simulated model and test specimen

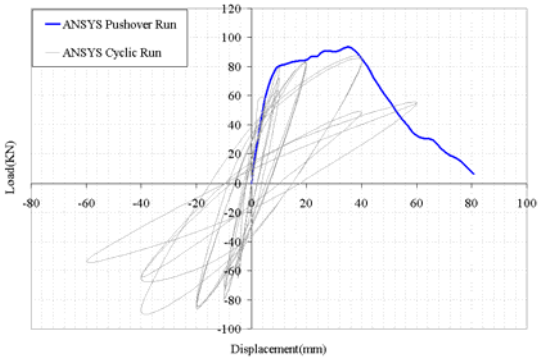

Fig. 9. Comparing Pushover and Cyclic curves for the model

Figure 10 presents the axial strain of the beam after failure for the F.E. model. As shown in this figure, concrete is crushed at a strain of -0.0064, and all steel bars (as one can see from Fig. 2) are in strain hardening zone at a strain of 0.0435.

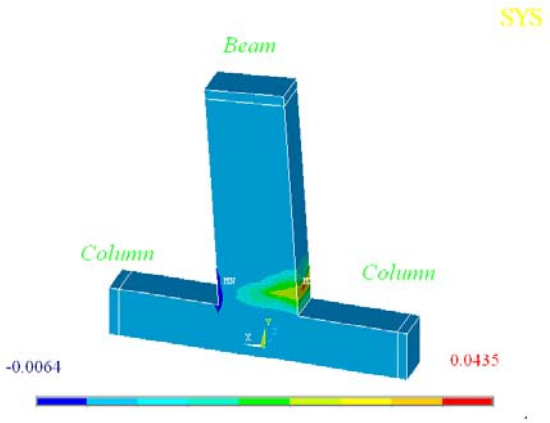

Fig. 10. A typical axial strains in the developed model

In crack patterns which are shown in Fig. 11a the red lines represent the cracks at the end of the experiment. Comparing these cracks with those developed in a real test model, Fig. 11b shows good matching between the behavior of the real specimen and the simulated model.

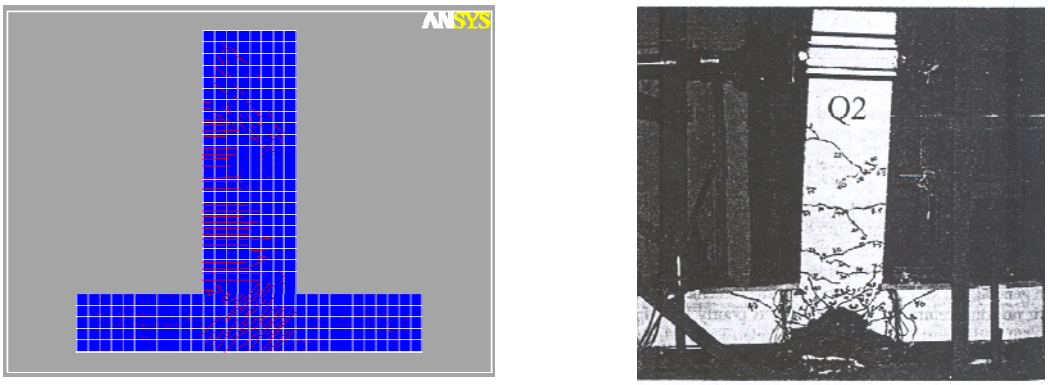

(a) (b)

Fig. 11. (a) Crack pattern in simulated model (Pushover analysis),
(b) Real specimen after testing

3. VIRTUAL TEST (SIMULATION) SETUP

All considered joints are designed to comply with the specifications of ACI design manual for high seismic regions [4].

a) Model generation

From six series of models (which are developed based on two classes of models defined in Table 1 and four different joint transverse steel ratios, 24 different F.E. models called ***B11*** through ***C34*** with specified configurations provided in Tables 1 and 2 were generated.

Table 1. Column dimensions and reinforcements for two classes of models

Class of Model	Column Cross Section (mm^2)	Column Steel Ratio	Beam Tension Steel ratio	Ties	Stirrups
B	300×300	0.04	0.012	Φ14 @80mm	Φ10 @80mm
C	300×450	0.04	0.012	2Φ12 @80mm	Φ10 @80mm

Table 2. Joint reinforcement for different models

Model Series	Beam Cross Section (mm^2)	Joint Transverse Steel Ratio			
		Type1	*Type2*	*Type3*	*Type4*
B1	300×300	0.017	0	0.005	0.030
B2	300×450	0.017	0	0.005	0.030
B3	300×600	0.017	0	0.005	0.030
C1	450×300	0.006	0	0.005	0.015
C2	450×450	0.006	0	0.005	0.015
C3	450×600	0.006	0	0.005	0.015

In naming the developed models, for instance ***B21***, defines a model belonging to class ***B*** (Table 1) with beam dimensions $300^{mm}\times450^{mm}$ given in the second column of Table 2 and type 1 for joint transverse steel ratio given in the third column of Table 2.

Figure 12a shows the characteristics of these generated models, such as geometry, dimensions and transverse and longitudinal bars.

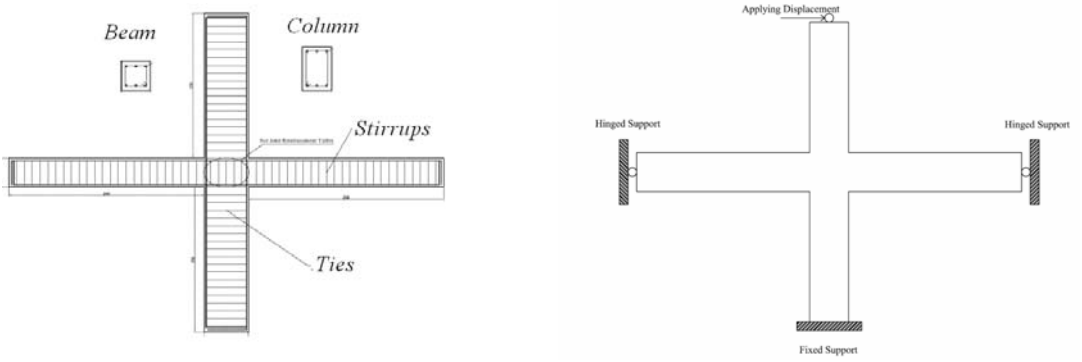

(a) (b)

Fig. 12. A typical model (a) Characteristics of model, (b) Supports conditions

b) Support conditions

For all models, support conditions are defined to be capable of simulating lateral loading for real seismic loads. As shown in Fig. 12b joint supports are pinned on three sides and fixed on the fourth side.

c) Loading

Two different loading patterns are applied to the simulated models. Both patterns are displacement control type. The first pattern is pushover loading type where displacement increases up to failure of connection.

The second pattern is cyclic loading in which displacement increases in two different directions at the magnitude of 0.02 meters per each step and remains the same for three cycles per each step. Except for the

first two steps where displacement increases by 0.01 meters per step. Figures 13a and 13b show loading patterns.

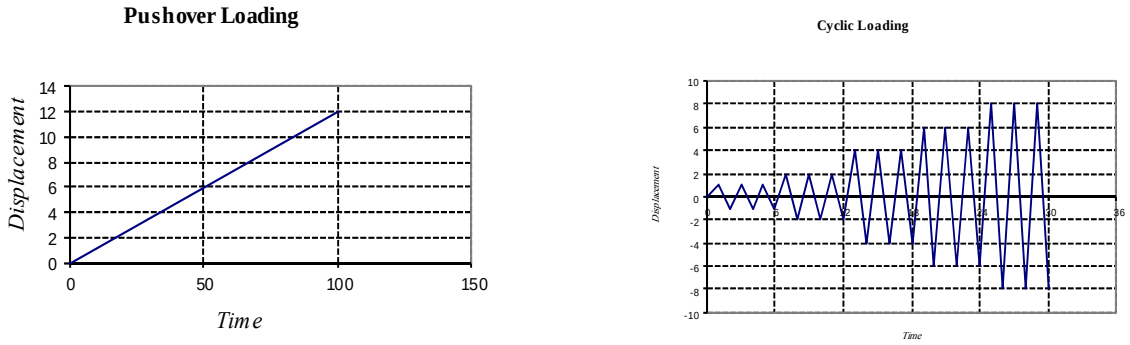

(a) (b)

Fig. 13. Virtual loading applied to the models: (a) Pushover loading, (b) Cyclic loading

d) Analysis

Two different types of analysis, which depend on loading patterns, are used to analyze the models. Type one is used for pushover analysis and presents results of pushing the structure fin several steps, from beginning to failure. In type two a transient dynamic load with push and pull cycles is applied as cyclic loading. Results are presented at three points in each cycle, maximum point, minimum point and onset point (where displacement is zero).

e) Meshing

Mesh generation is one of the influential steps that affects the accuracy and precision of results. For regular prismatic bodies, eight-node cube solid elements are suitable to model a joint structure. Generally, for this type of element, accuracy depends on the size of the elements. By a lengthy process for finding a relatively efficient mesh size to get the best precision with minimum computational time, we found that a 50 *mm* cubic element is a suitable choice.

4. VIRTUAL TEST (SIMULATION) RESULTS

Out of all analysis outputs available in literature, we chose few appropriate results so as to be able to investigate the importance and performance of the following concepts: (*i*) load-displacement curves for pushover and cyclic loadings, (*ii*) drawing over-strength curves and (*iii*) determining displacement ductility, μ, for joints. In the following section these concepts will be discussed in more detail.

a) Loading effect

The performance of a joint and mainly its ultimate strength and displacement ductility under cyclic and pushover tests are compared and discrepancies are verified. Both pushover and cyclic load-displacement curves are shown on the same graph. These graphs for some models are shown in Fig. 14. Backbone curves for cyclic–hysteretic loops are compared with pushover curves. By studying results for all models it can be seen that for most models, the hysteretic-loop-backbone curves move closely to pushover curves except for ***B1i*** and ***C1i*** models (i=1, …, 4) which are one third of all considered models. For the remaining two thirds of models the difference is relatively small with an average of 6.58% (minimum of zero and maximum of 14%). It is almost a common error in most laboratory tests.

But for models ***B1i*** and ***C1i*** the average and maximum amounts of error are 25.1% and 32%, respectively. Such an error is not acceptable, but it might be justified by the beam heights for models ***B1i*** and ***C1i*** which are smaller than the heights of the beams in other models. So, in push and pull cycles crack propagation will increase faster than the other models. This conclusion can be raised from the fact that the reinforced confined core is placed in the middle of a beam and does not provide enough strength to prevent crack propagation.

Next, we study the displacement ductility, μ, which is defined as the ratio of the ultimate displacement of the model, δu (where load decreases more than 15%), to yielding displacement, δy (which is defined by equalized perfect elastic-plastic curve). To determine displacement ductility, the displacement from equating pushover and backbone curves must be equated to displacement from elastic perfect plastic diagrams. The displacement ductility of all models are determined and given in Tables 3 and 4. Ultimate displacements of models are compared for two considered loading patterns in Tables 6, 8 and 10. A comparison between ultimate loads can be observed in Tables 5, 7 and 9.

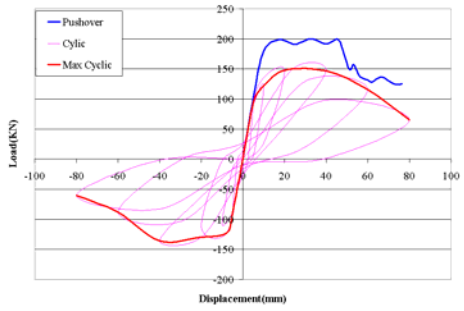

(a) Model ***B11***

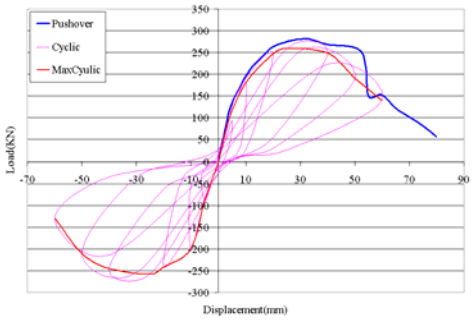

(d) Model ***C21***

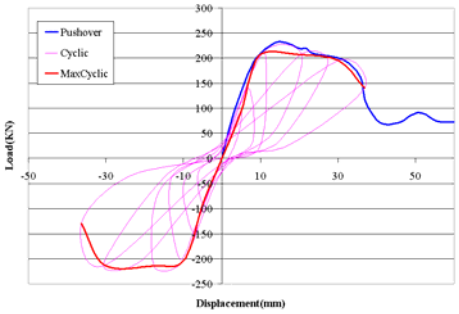

(b) Model ***B22***

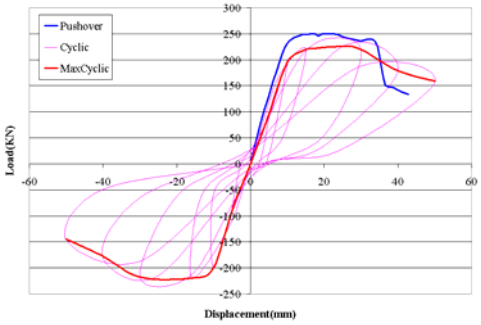

(e) Model ***C22***

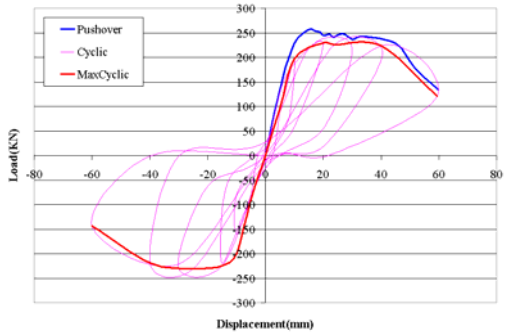

(c) Model ***B23***

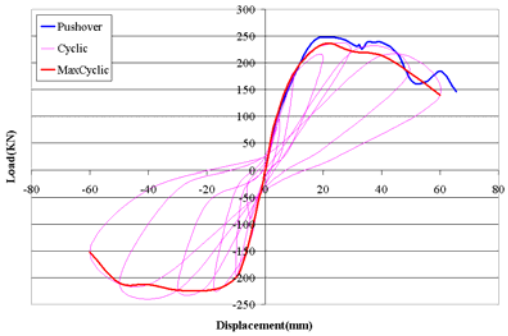

(f) Model ***C23***

Fig. 14. Comparing load-displacement curves from Pushover and Cyclic analysis

Table 3. Results of virtual tests for Pushover loading

Pushover Analysis

Model	ρ_s	Moment capacity ratio M_R	*Yield disp. (mm)*	*Ult. disp. (mm)*	μ	$(V_{ult})_{col}$ *(kN)*
B11	0.017	3.80	17.5	49.0	2.8	200
B12	0.000	3.80	17.4	33.0	1.9	192
B13	0.005	3.80	17.6	44.0	2.5	201
B14	0.030	3.80	18.2	51.0	2.8	219
B21	0.017	1.87	18.0	56.0	3.1	253
B22	0.000	1.87	14.1	34.0	2.4	250
B23	0.005	1.87	15.5	45.0	2.9	258
B24	0.03	1.87	15.7	55.0	3.5	273
B31	0.017	1.08	15.0	26.0	1.7	250
B32	0.000	1.08	16.7	20.0	1.2	250
B33	0.005	1.08	14.0	22.4	1.6	257
B34	0.030	1.08	14.0	25.2	1.8	273
C11	0.006	3.80	20.0	41.0	2.1	213
C12	0.000	3.80	17.6	30.0	1.7	212
C13	0.005	3.80	18.6	36.3	1.9	215
C14	0.015	3.80	17.3	45.0	2.2	220
C21	0.006	1.88	21.3	51.0	2.4	282
C22	0.000	1.88	15.6	31.3	2.0	230
C23	0.005	1.88	19.6	45.0	2.3	249
C24	0.015	1.88	20.4	49.0	2.4	293
C31	0.006	1.08	13.8	25.0	1.8	220
C32	0.000	1.08	10.0	15.0	1.5	212
C33	0.005	1.08	10.0	18.0	1.8	225
C34	0.015	1.08	14.0	26.6	1.9	231

Table 4. Results of virtual tests for Cyclic loading

Cyclic Analysis

Model	ρ_s	*Moment capacity ratio* M_R	*Yield disp. (mm)*	*Ult. disp. (mm)*	μ	$(V_{ult})_{col}$ *(kN)*
B11	0.017	3.80	17.5	55.0	3.1	147
B12	0.000	3.80	17.4	40.0	2.3	150
B13	0.005	3.80	17.6	48.0	2.7	149
B14	0.030	3.80	18.2	60.0	3.3	149
B21	0.017	1.87	18.0	56.0	3.1	230
B22	0.000	1.87	14.1	38.0	2.7	226
B23	0.005	1.87	18.0	46.0	2.6	230
B24	0.030	1.87	18.0	56.0	3.1	235
B31	0.017	1.08	15.0	26.0	1.7	241
B32	0.000	1.08	16.7	26.0	1.6	230
B33	0.005	1.08	16.0	26.0	1.6	241
B34	0.030	1.08	14.0	28.0	2.0	234
C11	0.006	3.80	20.0	47.2	2.4	164
C12	0.000	3.80	17.6	37.0	2.1	162
C13	0.005	3.80	18.6	44.0	2.4	164
C14	0.015	3.80	17.3	44.0	2.5	167
C21	0.006	1.88	21.3	48.0	2.3	259
C22	0.000	1.88	15.6	32.0	2.1	210
C23	0.005	1.88	19.6	44.0	2.2	235
C24	0.015	1.88	20.4	52.0	2.5	259
C31	0.006	1.08	13.8	29.0	2.1	215
C32	0.000	1.08	12.0	21.0	1.8	203
C33	0.005	1.08	14.0	27.0	1.9	221
C34	0.015	1.08	14.0	26.0	1.9	215

Table 5. Comparing ultimate loads results for model ***B1i*** and ***C1i*** (i=1, …, 4)

Models	V_{ult} *Push. (kN)*	V_{ult} *Cyclic (kN)*	Difference (*kN*)	Difference Percentage %
B11	200	147.4	52.6	0.26
B12	192	149.5	42.5	0.22
B13	201	149.0	52.0	0.26
B14	219	149.0	70.0	0.32
C11	213	164.3	48.7	0.23
C12	212	162.0	50.0	0.24
C13	215	164.0	51.0	0.24
C14	220	166.5	53.5	0.24

Table 6. Comparing displacement results for model ***B1i*** and ***C1i*** (i=1, …, 4)

Models	Δ_{ult} *Push. (mm)*	Δ_{ult} *Cyclic (mm)*	Difference (*mm*)	Difference Percentage %
B11	49.0	55.0	-6.0	-0.12
B12	33.0	40.0	-7.0	-0.21
B13	44.0	48.0	-4.0	-0.09
B14	51.0	60.0	-9.0	-0.18
C11	41.0	47.2	-6.2	-0.15
C12	30.0	37.0	-7.0	-0.23
C13	36.3	44.0	-7.7	-0.21
C14	45.0	44.0	1.0	0.02

Table 7. Comparing ultimate loads results for model ***B2i*** and ***C2i*** (*i*=1, …, 4)

Models	V_{ult} *Push. (kN)*	V_{ult} *Cyclic (kN)*	Difference (*kN*)	Difference Percentage %
B21	253	230.0	23.0	0.09
B22	250	226.0	24.0	0.10
B23	258	230.0	28.0	0.11
B24	273	235.0	38.0	0.14
C21	282	259.0	23.0	0.08
C22	230	210.0	20.0	0.09
C23	249	235.0	14.0	0.06
C24	293	259.0	34.0	0.12

Table 8. Comparing displacement results for model ***B2i*** and ***C2i*** (*i*=1, …, 4)

Models	Δ_{ult} *Push. (mm)*	Δ_{ult} *Cyclic (mm)*	Difference (*mm*)	Difference Percentage %
B21	56.0	56.0	0.0	0.00
B22	34.0	38.0	-4.0	-0.12
B23	45.0	46.0	-1.0	-0.02
B24	55.0	56.0	-1.0	-0.02
C21	51.0	48.0	3.0	0.06
C22	31.3	32.0	-0.8	-0.02
C23	45.0	44.0	1.0	0.02
C24	49.0	52.0	-3.0	-0.06

Table 9. Comparing ultimate loads results for model ***B3i*** and ***C3i*** (*i*=1, …, 4)

Models	V_{ult} *Push. (kN)*	V_{ult} *Cyclic (kN)*	Difference (*kN*)	Difference Percentage %
B31	250	241.0	9.0	0.04
B32	250	230.0	20.0	0.08
B33	257	241.0	16.0	0.06
B34	273	234.0	39.0	0.14
C31	220	215.0	5.0	0.02
C32	212	203.0	9.0	0.04
C33	225	221.0	4.0	0.02
C34	231	215.0	16.0	0.07

Table 10. Comparing displacement results for model ***B3i*** and ***C3i*** (*i*=1, …, 4)

Models	Δ_{ult} *Push. (mm)*	Δ_{ult} *Cyclic (mm)*	Difference (*mm*)	Difference Percentage %
B31	26.0	26.0	0.0	0.00
B32	20.0	26.0	-6.0	-0.30
B33	22.4	26.0	-3.6	-0.16
B34	25.2	28.0	-2.8	-0.11
C31	25.0	29.0	-4.0	-0.16
C32	15.0	21.0	-6.0	-0.40
C33	18.0	27.0	-9.0	-0.50
C34	26.6	26.0	0.6.0	0.020

From these tables one can conclude that; (*i*) The best result for ultimate displacement with the minimum variation occurs for models ***B2i*** and ***C2i***, with 4% (in average) difference for ductility (maximum 12%) which is good enough to accept the results. The largest differences belong to models ***B32***, ***C32*** and ***C33***. The error for these models can be justified by post yielding analysis error. For other models these differences vary between 0 and 23% with an average of 12.8% that could be acceptable.

(*ii*) Ultimate strengths which are the peak points of load–displacement curves are summarized in Tables 3 and 4 for all models and both cyclic and pushover loads. As it can be seen, there is no significant changes in magnitudes of ultimate strengths due to any changes in joint dimensions or joint reinforcement for both cyclic and pushover loadings. This can be explained by the failure mode of the joint and modeling characteristics. For example, if failure mode is a flexural type, then joint core reinforcement might not participate in joint strength, besides it is also possible that the model is not capable to simulate the confinement of the joint core reinforcement, completely. This phenomenon needs more investigation. The best achieved strength among all models belongs to models ***B2i*** and ***C2i*** which have the same cross sections for both beams and columns.

(*iii*) The computed displacement ductilities, μ, are provided in the sixth column of Tables 3 and 4. The best achieved ductility for each series of models belongs to ***Bi4*** and ***Ci4*** models (*i*=1, 2, 3). Models ***Bi1***, ***Ci1*** (*i*=1, 2, 3) show good ductilities. Models ***Bi2***, ***Ci2*** and ***Bi3***, ***Ci3*** have a ductility problem. In general, if computed ductility of a model is between 1.2 to 3.11 it is not good enough.

(*iv*) Variations in ultimate strength and displacement with respect to the change in joint reinforcement for some models can be seen in Fig. 15. For almost all models with the same beam and column sizes, both ultimate strength (peak of the curve) and ultimate displacement (the point of 15% decrease in strength) move up by increasing the joint core reinforcement (ρ_s) and these models demonstrate better behavior. Although the increase of ultimate strength is not significant, there is considerable variation in ultimate displacement. The area under the curve is proportionally varying by the amount of joint reinforcement. In general, it can be concluded that, an increase in joint reinforcement will improve joint performance (ultimate strength, displacement ductility and energy dissipation).

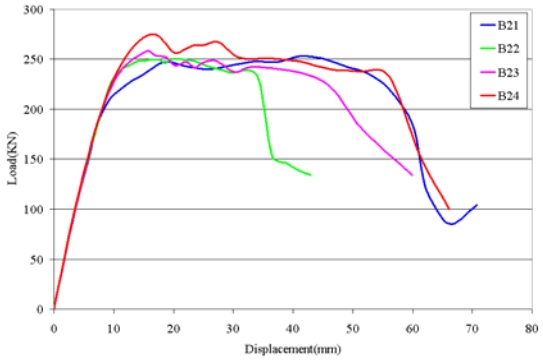

(a) Pushover loading, Model Series: ***B2***

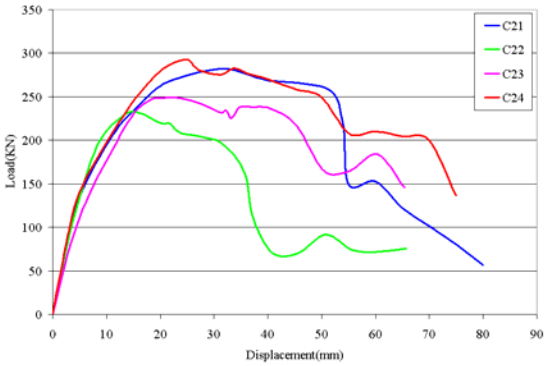

(c) Pushover loading, Model Series: **C2**

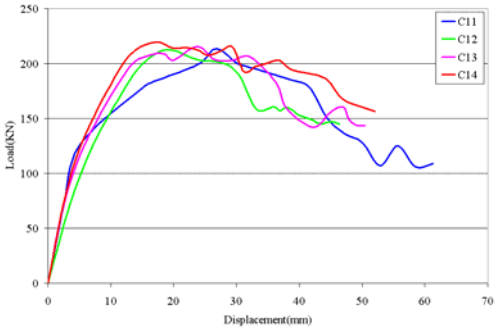

(b) Pushover loading, Model Series: ***C1***

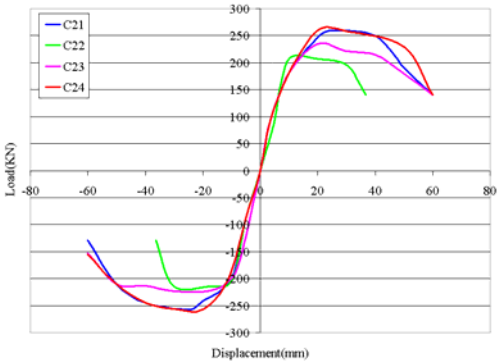

(d) Cyclic loading, Model Series: ***C2***

Fig. 15. Effect of joint reinforcement on joint behavior

b) Over-strength factors

Increasing ultimate strength with respect to nominal strength proposed by ACI code is called over-strength factor. For example, for beam bending, code criterion proposes M_{pr} for ultimate strength to be computed by considering tensile stress of $1.25F_y$ in rebars and compressive strain of 0.003 in concrete. Now if the flexural capacity of the beam is M_u, then over-strength factor for beam bending is defined as $B.O.S.F=M_u/M_{pr}$.

For joint shearing strength the code criterion defines $V_c=9A_j v_c$ as joint maximum shear strength. The joint shear over-strength factor will be $J.O.S.F=V_u/V_j$, where V_u is the failure shear capacity of the joint.

In general, by computing the over-strength factors for different members of a structure, one may conclude that:

1- The magnitude of the over-strength factor can be used to determine code safety factors, which helps to improve designing procedure.
2- By comparing the over-strength factors of different elements of a structure, weak links or critical points vulnerable to failure may be found.

Figure 16 shows over-strength factor curves for different members of some models, which are beam bending overstrength factor (*B.O.S.F.*), column bending overstrength factor (*C.O.S.F.*), joint vertical and horizontal shear overstrength factor (*J.O.S.F.*). Where joint vertical shear is the shear that is caused by column end moments and joint horizontal shear is the shear that is caused by beam end moments. The

selected models for investigating the trend of these parameters are models ***B11***, ***B21***, ***B31***, ***C11***, ***C21*** and ***C31***.

B11 *pushover loading:* Joint vertical shear in this model increases up to more than twice the code demand. Beam bending over-strength factor reaches 1.5 times M_{pr}. An increase in over-strength factor (*O.S.F.*) shows that joint vertical section and beam ends have greater forces than column ends and joint horizontal section. This behavior can be explained by any decrease in beam height. Figure 16a shows the over-strength factor curves for model ***B11***.

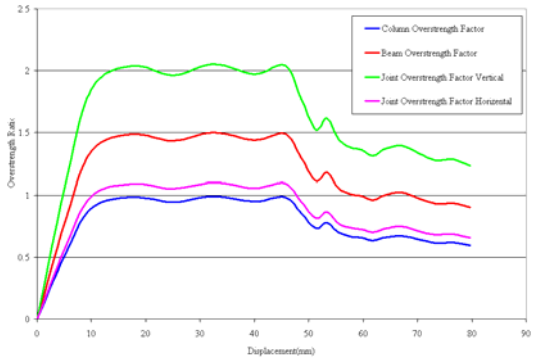

(a) Pushover analysis, model ***B11***

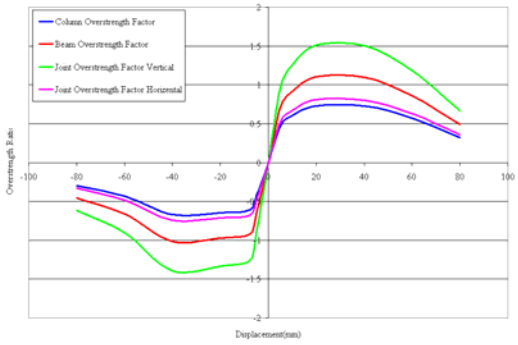

(d) Cyclic analysis, model ***B21***

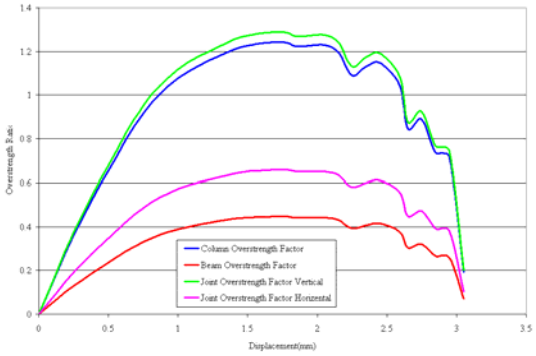

(b) Pushover analysis, model ***B31***

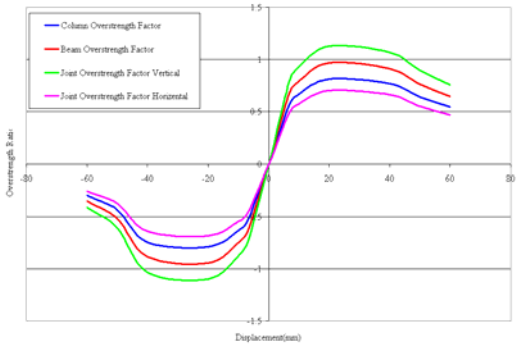

(e) Cyclic analysis, model ***C21***

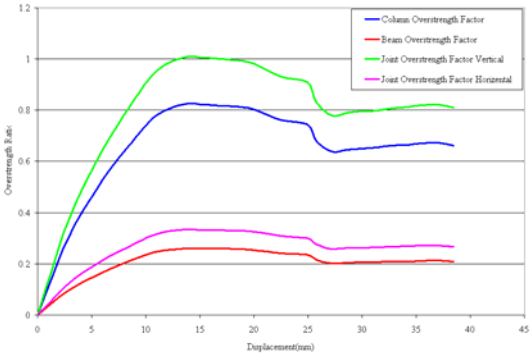

(c) Pushover analysis, model ***C31***

Fig. 16. Over-strength factor for some models

B11 *cyclic loading:* Cyclic back-bone curves for *O.S.F* follows almost similar trends as pushover loading causes (Figure not provided). But there is about 25% difference in results from these two types of loadings. Regardless of error, dynamic cyclic loading yields smaller magnitudes due to the nature of

dynamic loading. In general, dynamic loading reduces structural strength that might be due to material properties, increasing crack propagation and impact effect.

For almost all models the same trend for both types of loading is observed. Therefore, in the following section, the results from pushover analysis will not be discussed.

B21*:* Vertical joint shear *O.S.F* in this model increases up to 1.75 times the code shear capacity, V_c. For other models, *O.S.F* bounded to 1.25 times the code capacities.

B31*:* The magnitudes of *O.S.F.* for this model are 1.3 for vertical joint shear and 1.25 for column bending. It can be concluded that in this model corresponding capacities are close to code provisions. It might have arisen from the fact that beam height is larger than column's depth. Figure 16b shows *O.S.F.* curves from pushover loading of model ***B31***.

C11*:* Beam height in this model is the same as ***B11*** which is smaller than column's depth (Figure not provided). Similarly *O.S.F.* is greater than two other "***C***" models, ***C21*** and ***C31***. Joint vertical shear *O.S.F* increased up to 1.5 times V_c.

C21*:*As expected increasing beam height causes decreasing joint vertical shear *O.S.F.* to 1.3 in ***C21*** model for pushover loading and 1.2 for cyclic loading. Figure 16e shows *O.S.F* curves for ***C21***.

C31*:* A significant reduction in *O.S.F* can be seen in this model. Maximum *O.S.F* is joints vertical shear that has the magnitude of 1.0. It means the joint will fail before developing and reaching code capacities. Increasing beam height to over 1.3 times column's depth might be the main reason for this failure. Figure 16c shows *O.S.F* for model ***C31***.

Tables 11 through 13 summarized different *O.S.F.,* for all models. In these tables, M_R and V_R are two parameters used to verify values of over-strength factors.

1- M_R is the moment capacity ratio. It is defined as the ratio of the summation of column bending capacities to summation of beam bending capacities $\Sigma M_c/\Sigma M_b$ (given in Tables 3 and 4.

2- V_R is the shear capacity ratio. This parameter is defined as the relation between shear capacity of a joint corresponding to code criterion, and maximum shear of the joint caused by member end moments. This parameter is determined by the following equations.

$$V_R = \frac{9A_j v_c}{V_j} = \frac{9A_j v_c}{\left(\frac{2M_b}{h_c}\right)} \qquad \text{or} \qquad V_R = \frac{9A_j v_c}{V_j} = \frac{9A_j v_c}{\left(\frac{2M_c}{h_b}\right)}$$

Tables 11 through 13 can be used to compare over-strength factors for all models computed for both pushover and cyclic analysis.

Table 11. Over-strength factors, Pushover loading

Pushover Analysis				
Model	Beam *O.S.F* $(\frac{M_B}{M_{pr}})$	Column *O.S.F* $(\frac{M_C}{M_{pr}})$	Joint *O.S.F* $(\frac{V_j}{V_r})$ Vertical	Joint *O.S.F* $(\frac{V_j}{V_r})$ Horizontal
B1	0.99	1.50	2.05	1.10
B2	1.25	0.94	1.73	0.93
B3	1.24	0.45	1.29	0.66
C1	1.05	1.26	1.47	0.91
C2	1.06	0.70	1.29	0.69
C3	0.82	0.26	1.00	0.33

Table 12. Over-strength factors, Cyclic loading

Cyclic Analysis				
Model	Beam *O.S.F* $(\frac{M_B}{M_{pr}})$	Column *O.S.F* $(\frac{M_C}{M_{pr}})$	Joint *O.S.F* $(\frac{V_j}{V_r})$ Vertical	Joint *O.S.F* $(\frac{V_j}{V_r})$ Horizontal
B1	0.73	1.10	1.50	0.81
B2	1.14	0.85	1.58	0.84
B3	1.19	0.43	1.24	0.63
C1	0.81	0.97	1.13	0.70
C2	0.97	0.64	1.19	0.63
C3	0.80	0.26	0.99	0.33

Table 13. Over-strength factors, verifying

	$9A_j\nu_c$ (*kN*)	V_j (*kN*)	V_R	*O.S.F* Joint Shear	*O.S.F* Beam Mom.	*O.S.F* Column Mom.	Joint Shear Safety Factor
B1	486	360	1.35	2.05	1.50	0.99	2.05
B2	730	712	1.03	1.73	0.94	1.25	N/A (1.73)
B3	972	1690	0.58	1.29	0.45	1.24	1.29
C1	730	530	1.38	1.47	1.26	1.05	1.47
C2	1090	1080	1.01	1.29	0.70	1.06	N/A (1.29)
C3	1460	1640	0.89	1.00	0.26	0.82	1.00

5. CONCLUSION

A detailed process of developing and verifying a robust F.E. model for a RC beam column connection is presented. After modeling many joints and post processing the results, the conclusions are summarized as follows:

a) Simulation Characteristics:

1- **ANSYS** can be used for both modeling and detecting damage in an existing RC structure. But in order to be able to observe a specific behavior from the model, the required modeling parameters must be defined and adjusted properly.

2- Both cyclic dynamic and pushover results of the considered F.E. models show acceptable matching with the real test data.

3- Pushover static test presents up to 15% increase in strength compared to cyclic dynamic test.

b) Effect of joint reinforcement:

1-The joint core reinforcement (ρ_s) improves joint seismic performance.

2- The joint reinforcement significantly affects the displacement ductility and post failure behavior of a connection.

3- Increasing joint reinforcement does not significantly affect joint ultimate strength.

c) Moment Capacity Ratios and Shear Capacity Ratios:

1- Models with greater (significantly more than 1.0) shear capacity ratios, V_R, and moment capacity ratios, M_R, have the capabilities to resist forces with magnitudes 70% up to 100% more than code requirements.
2- Beams in models with moment capacity ratios, M_R, significantly greater than 1.0, resist forces more than their expected capacities assigned by the design code.
3- For models with moment capacity ratios less than 1.2 (which is code requirement), and shear capacity ratios less than 1.0, the *O.S.F.* decreases and failure occurs at *O.S.F* about 1.0.
4- For models with moment capacity ratios greater than 1.2 and shear capacity ratio more than 1.0, ultimate strength is 40% to 50% more than code requirements, which makes them safe.

Finally, it must be mentioned that this research was not a comprehensive study and simulated outputs cannot be considered as conclusive results. To verify these conclusions further numerical and experimental investigations are required.

REFERENCES

1. Hanson, N. W. & Conner, H. W. (1967). Seismic resistance of reinforced concrete beam-column joints. *Proceedings, ASCE*, Vol. 93(ST5), pp. 533-560.
2. Hanson, N. W. (1971). Seismic resistance of concrete frames with Grade 60 reinforcement. *Proceedings*, *ASCE*, Vol. 97(ST6), pp. 1685-1700.
3. ACI-ASCE Committee352. (1976). Recommendations for design of beam-column joints in monolithic reinforced concrete structures. *ACI 352R-76*, American Concrete Institute, Detroit, U.S.A.
4. ACI-ASCE Committee352. (2002). Recommendations for design of beam-column joints in monolithic reinforced concrete structures. *ACI 352R-02*, American Concrete Institute, Detroit, U.S.A.
5. Murty, C. V. R., Rai, D. C., Bajpai, K. K. & Jain, S. K. (2003). Effectiveness of reinforcement details in exterior reinforced concrete beam-column joints for earthquake resistance. *ACI Structural Journal*, Vol. 100, No. 2, pp. 149-156.
6. Megget, L. M. (1974). Cyclic behavior of exterior reinforced concrete beam-column joints. *Bulletin of the New Zealand National Society for Earthquake Engineering*, Vol. 7, No. 1, pp. 27-47.
7. Paulay T., Park, R. & Priestley, M. J. N. (1978). Reinforced concrete beam-column joints under seismic actions. *ACI Structural Journal*, Vol. 75, No. 11, pp. 585-593.
8. Paulay, T. & Scarpas, A. (1981). The behavior of exterior beam-column joints. *Bulletin of the New Zealand National Society for Earthquake Engineering*, Vol. 14, No. 3, pp. 131-144.
9. Durrani, A. J. & Wight, J. K. (1985). Behavior of interior beam-to-column connections under earthquake type loading. *ACI Structural Journal*, Vol. 82, No. 3, pp. 343-349.
10. Ehsani, M. R. & Wight, J. F. (1985). Exterior reinforced concrete beam-to-column connections subjected to earthquake-type loading. *ACI Structural Journal*, Vol. 82, pp. 492-499.
11. Kitayama, K., Otani, S. & Aoyama, H. (1987). Earthquake resistant design criteria for reinforced concrete interior beam-column joints. *Proceedings of Pacific Conference on Earthquake Engineering*. Wairakei, New Zealand, Agust 5-8, Vol. 1, pp. 315-326.
12. Tsonos, A. G, Tegos, I. A. & Penelis, G. (1992). Seismic resistance of type 2 exterior beam-column joints reinforced with inclined bars. *AIC Structural Journal*, Vol. 89, pp. 3-12.
13. Agbabian, M, Higazy, E. M. & Abdel-Ghaffar, A. M. (1994). Experimental observations on the seismic shear performance of RC beam-to-column connections subjected to varying axial column force. *Earthquake Engineering and Structural Dynamics*, Vol. 23, pp. 859-876.
14. Hakuto, S, Park, R. & Tanaka, H. (2000). Seismic load tests on interior and exterior beam-column joints with substandard reinforcing details. *ACI Structural Journal*, Vol. 97, No. 1, pp. 11-25.

15. Hwang, S. J., Lee, H. J. & Wang, K. C. (2004). Seismic design and detailing of exterior reinforced concrete beam-column joints. *13th World Conference on Earthquake Engineering*. Vancouver, Canada, August 1-8, Paper No. 397.
16. Hwang, S. J., Lee, H. J., Liao, T. F., Wang, K. C. & Tsai, H. H. (2005). Role of hoops on shear strength of reinforced concrete beam-column joints. *ACI Structural Journal*, Vol. 102, No. 3, pp. 445-453.
17. Tsonos, A. G. (2007). Cyclic load behavior of reinforce concrete beam-column sub-assemblages of modern structures. *ACI Structural Journal*, Vol. 104, 4), pp.468-478.
18. Bindhu, K. R., Sukumar, P. M. & Jaya, K. P. (2009). Performance of exterior beam-column joints under seismic type loading. *ISET Journal of Earthquake Technology*, Vol. 46, No. 2, pp. 47-64.
19. Bindhu, K. R. & Sreekumar, K. J. (2011). Seismic resistance of exterior beam-column joint with diagonal collar stirrups. *International Journal of Civil and Structural Engineering*, Vol. 2, No. 1, pp. 160-175.
20. Asha, P. & Sundararajan, R. (2012). Seismic behavior of exterior beam-column joints with square spiral confinement. *Asian Journal of Civil Engineering* (*Building and Housing*), Vol. 13, No. 4, pp. 571-583.
21. Mostofinejad, D. & Talaeitaba, S. B. (2006). Finite element modeling of RC connections strengthened with FRP laminates. *Iranian Journal of Science and Technology*, *Transaction B*, Vol. 30, No. B1, pp. 21-30.
22. Dalalbashi Esfahani, A., Mostofinejad, D., Mahini, S. & Ronagh, H. R. (2011). Numerical investigation on the behavior of FRP retrofitted RC exterior beam-column joints under cyclic loads. *Iranian Journal of Science and Technology, Transactions of Civil and Environmental Engineering*, Vol. 35, No. C1, pp. 35-50.
23. Sharbatdar, M. K., Dalvand, A. & Hamze-Nejadi, A. (2013). Experimental and numerical assessment of FRP stirrups distance on cyclic behavior of RC joints. *Iranian Journal of Science and Technology, Transactions of Civil Engineering*, Vol. 37, No. C^+, pp. 367-381.
24. Hadigheh, S. A., Maheri, M. R. & Mahini, S. S. (2013). Performance of weak-beam, strong-column RC frames strengthened at the joints by FRP. *Iranian Journal of Science and Technology, Transactions of Civil Engineering*, Vol. 37, No. C1, pp. 33-51.
25. Arslan, M. H. & Gulay, F. G. (2009). Numerical study on seismic behavior of precast concrete connection zone. *Iranian Journal of Science and Technology, Transaction B*, Vol. 33, No. B1, pp. 123-127.